Radio frequency interference detection and mitigation techniques using data from EcoSAR 2014 Flight Campaign

Batuhan Osmanoglu, NASA/Goddard Space Flight Center, Greenbelt, MD 20771
Rafael F. Rincon, NASA/Goddard Space Flight Center, Greenbelt, MD 20771
SeungKuk Lee, USRA, NASA/Goddard Space Flight Center, Greenbelt, MD 20771
Temilola Fatoyinbo, NASA/Goddard Space Flight Center, Greenbelt, MD 20771
Tobias Bollian, USRA, NASA/Goddard Space Flight Center, Greenbelt, MD 20771

Abstract

Radio frequency interference (RFI) has strong influence on wide band airborne radar systems, especially operaing at L-band (1-2 GHz) or lower frequencies. EcoSAR is a P-band digital beamforming radar system, and RFI has to be removed from raw echoes to obtain science quality data. In this paper we describe the current methodology used to tackle RFI with EcoSAR, and provide an example on its performance. Finally, we discuss the advantages and disadvantages of the method and mention potential improvements.

1 Introduction

Radio frequency interference occurs as a result of acquisition of unwanted radio signals together with the signal of interest. Unwanted radio signals can be of natural sources (e.g. sun, lightning), which generally occur at low frequencies (100 to 10,000 Hz) [1]. Anthropogenic signals occur due to either unlicensed use of radio waves or due to operation of a wide-band system, which goes beyond the spectrum allocations of International Telecommunications Union (ITU). In any case, RFI degrades the performance of the receiver and results in reduced signal to noise ratio (SNR) [2].

EcoSAR is a wideband (up to 200 MHz) radar system operating at the P-band, 435 MHz center frequency. This band is routinely used by short-range amateur radios, wind profilers, and TV stations each of which have 6 MHz bandwidth. ITU allocation for space-borne radar systems at P-band (435 MHz) is only 6 MHz, therefore, most of EcoSAR operating band falls outside the allocated spectrum [3]. However, even within the allocated 6 MHz band, EcoSAR data shows presence of RFI in Figure 1.

1.1 EcoSAR

EcoSAR is a quad-pol system with 32 independent antenna sub arrays (eight active sub arrays for each polarization) [3][4]. During the first EcoSAR flight campaign in 2014, data was collected in wide-beam imaging mode, with a single sub-array transmitting. This mode allows for imaging multiple ground swaths on both sides of the airplane [5].

EcoSAR utilizes several filters along its receive path to remove signals outside the transmit band. The antenna also behaves like a band-pass filter because it attains over 20 dB loss outside 335-535 MHz for V and 375-495 MHz in H polarizations. Just before the LNA a 300 MHz band-pass filter is located in the receive path, further eliminating signals outside the band (Figure 2). A 200 MHz filter is located just before the analog to digital converter (ADC). Finally, a digital filter is implemented in the
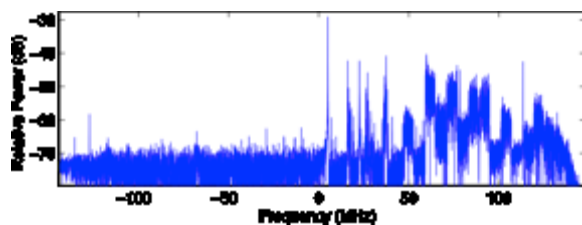

Figure 1 RFI measurement taken by EcoSAR with digital band-pass filter turned off. Center frequency is located at 0 MHz. Note the strong interference in the transmit band (-100, +100 MHz). The data is from a single channel, no beamforming or correction applied. The strongest RFI is at +5.116 MHz, at -29.09 dB.
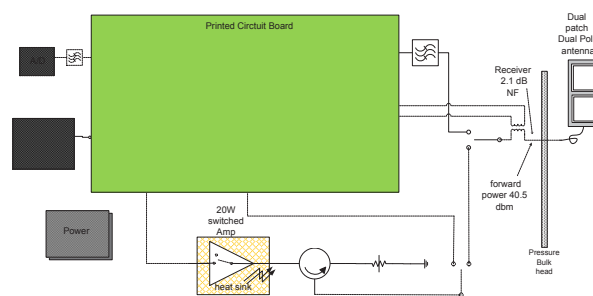

Figure 2 EcoSAR Transceiver block diagram. The A/D and DDS signal generator are realized inside the processor box. Pre- and post-LNA filters are shown.

FPGA, and can be operated at 36, 72 and 144 MHz bandwidths. The digital filter can also be turned off completely, leaving the 290 MHz bandwidth intact. These filters provide decent (> 60 dB) out-of-band signal suppression, but do little for RFI within the operating band.

2 Methods

We are currently working on two different in-band RFI removal methods. For the first method, a sniffing pulse is inserted instead of one of the transmitting pulses. Hence, the radar listens for the duration of one pulse repetition interval (PRI). This enables the detection of frequency bins affected by RFI in the absence of the radar signal. While detection in the presence of the SAR return requires RFI to be significantly stronger than a set threshold, this approach also detects less strong RFI. Figure 3 shows the averaged spectrum of a transmit pulse and a sniffing pulse. Few bins with RFI can easily be detected within the transmit pulse, but several bins are masked out by the radar signal itself. Also, most of the RFI spikes that are slightly stronger than the radar signal would be hard to detect in a less averaged, hence noisier, spectrum. Frequency bins are marked in the beamformed sniffing pulse spectrum. Then they are notched out in the transmit pulses to achieve RFI filtering. A consequence of this approach is the reduction of the effective pulse repetition frequency (PRF) at the cost of one transmit pulse or the increase of azimuth ambiguities and data throughput.

The second RFI removal technique we are working on utilizes the digital beamforming characteristic of the EcoSAR system. In this method, we beamform the received echo between -90 and +90 degrees in an effort to find the direction of the RFI signal. This can be achieved by

means of direction of arrival estimation algorithms as for example the Capon beamformer [6] or the MUSIC algorithm [7]. While the looking angle of the SAR return is positively correlated with fast time (Fig. 7), the look angle for a fixed RFI source is assumed to be fixed within one pulse. Once the angle has been estimated, a null is placed in the direction of the RFI, reducing the unwanted radar signal [8]. Because the EcoSAR antenna has eight elements, it has eight degrees of freedom, one of which is used for the main lobe, while the remaining 7 can be used to reduce directional RFI.

3 Results

Figure 4 presents imagery collected on March 27th, 2014 over the Andros Island, Bahamas, during the very first EcoSAR flight. The acquired image is affected with RFI as shown in Fig. 1. The focused image shows the signs of interference as bright lines across the image. The RFI filtered image is qualitatively better, even though some aberrations are still evident in the far range (bottom-right of the Fig. 4b). These aberrations are likely due to the leftover RFI after the filtering. Data collected on March 31st 2014 over Costa Rica is shown in Figure 5 before and after applying RFI filtering. Even though no artefacts are visible before filtering, the filtered image is less noisy and shows an increased image contrast. This can be contributed to the notching of many weak RFI sources that are detected with the sniffing pulse. The flight path for the
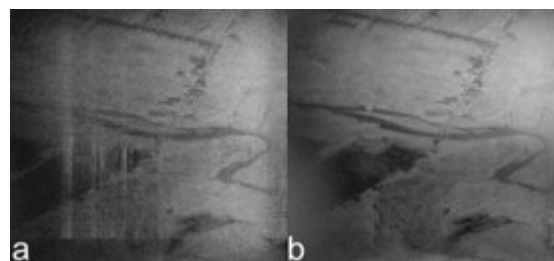
Figure 4 EcoSAR focused imagery over Andros Island, Bahamas in radar coordinates. Range is shown in horizontal and azimuth is shown in vertical axis. a. Focused 50 MHz imagery with RFI. b. RFI Filtered 30 MHz image.

Figure 5 EcoSAR focused imagery over Costa Rica in radar coordinates. Range is shown in vertical and azimuth is shown in horizontal axis. a. With RFI. b. After RFI filter.
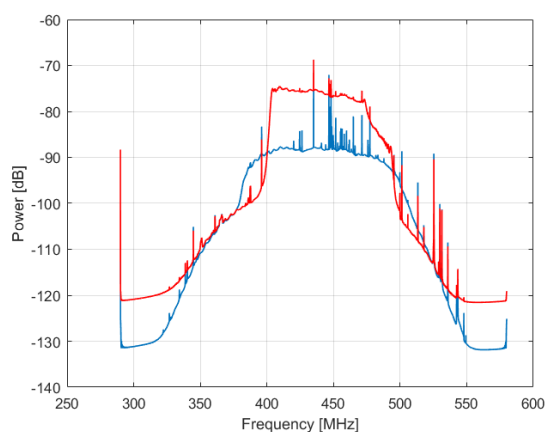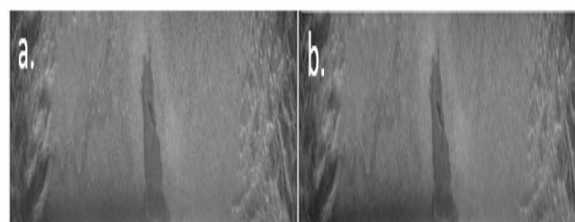

Figure 3 Averaged FFT spectrum of a transmitted SAR signal (red) and the radar operating in listening only mode (blue). Strong RFI peaks are present in both spectras, with multiple weaker interferences being masked by the SAR signal itself.
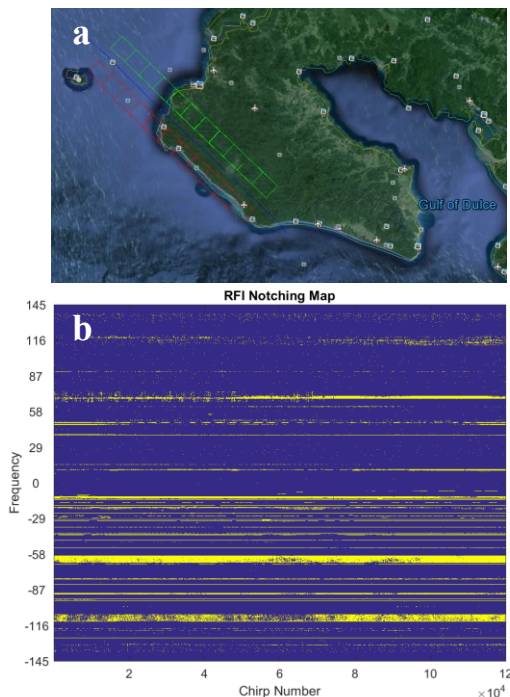
Figure 6: a) Flight track of data acquired in Costa Rica on March 31st 2014. b) Frequency bins masked as RFI in sniffing pulse in yellow and how they change with slow time.

Costa Rica scene is displayed in Figure 6 together with a map of the notched bins in frequency and in slow time.

4 Discussion

The main advantage of the current method is its operational simplicity, fast run-time and effectiveness in mitigating strong RFI. The algorithm is developed in the frequency domain and has a computational efficiency of O(N). On a single CPU desktop computer, it takes about 10 minutes to apply the RFI filter for a single EcoSAR image, consisting of eight channels and ~50,000 pulses.

On the other hand, the algorithm has two main drawbacks: 1- it removes signal together with the RFI; 2- it requires a sniffing pulse to eliminate RFI that is below the spectral power of the returned echo. However, for flown test sites in Costa Rica and the Bahamas, the frequencies affected by RFI seem to be changing slowly (Figure 6). Therefore, the amount of sniffing pulses could be reduced significantly to minimize drawbacks introduced by it. There are many other alternatives to RFI removal, generally improving performance with increased computational complexity [9]. An alternative method can be employed with digital beamforming by placing nulls in the direction of the RFI emitters [10][11]. An example with the MUSIC algorithm when estimating the direction of the two most dominant signals for the scene in Figure 5 is shown in Figure 7. Because the radar pulse was
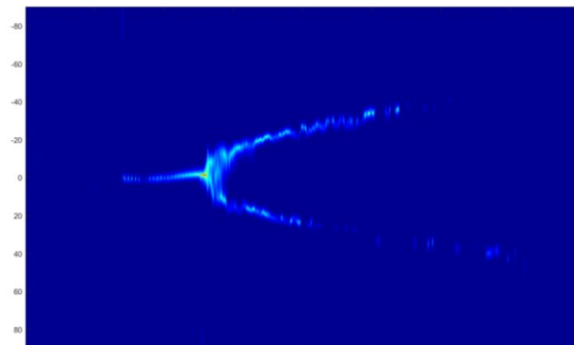

Figure 7: Angle of arrival of two most dominant sources using MUSIC algorithm for scene given in Figure 5. The radar transmit pulse illuminated both sides of the airplane. Hence, signals from both sides are received

transmitted with a single element without any directional antenna array gain, signals from both sides of the airplane are being received. As expected, incidence angles increase with fast time. This method could be used to determine the direction of beamforming nulls for the suppression of interfering sources.

5 Conclusions

In this paper we presented data collected during the first EcoSAR flight on March 27th, campaign in 2014, and analyze it in terms of RFI. We described a method to minimize the effects of the RFI using a sniffing pulse. The current implementation of the algorithm is computationally efficient due to its simplicity. On the other hand, it leaves the RFI weaker than the returned echo intact the sniffing pulse was introduced at the cost of one transmitting pulse. In the future, this can be avoided by minimizing the amount of sniffing pulses, as the frequency bins affected by RFI seem to be changing slowly with slow time.

Acknowledgements

References

[1] J.A. Marshall, B. Pine, and W. W.L. Taylor. "INSPIRE: A VLF Radio Project for High School Students." *The Physics Teacher* 45, no. 1 (2007): 42-45.

[2] C. S. Ruf, S. M. Gross, and S. Misra. "RFI detection and mitigation for microwave radiometry with an

agile digital detector." *Geoscience and Remote Sensing, IEEE Transactions on* 44, no. 3 (2006): 694-706.

[3] R. F. Rincon, T. Fatoyinbo, K. J. Ranson, G. Sun, M. Deshpande, M. Perrine, C. Du Toit et al. "Eco-SAR, An airborne P-band Polarimetric InSAR for the measurement of Ecosystem structure and biomass." In *EUSAR 2014; 10th European Conference on Synthetic Aperture Radar; Proceedings of*, pp. 1-4. VDE, 2014.

[4] Rafael F. Rincon, T. Fatoyinbo, G. Sun, K. J. Ranson, M. Perrine, M. Deshapnde, and Q. Bonds. "The ECOSAR P-band Synthetic Aperture Radar." In *Geoscience and Remote Sensing Symposium (IGARSS), 2011 IEEE International*, pp. 1512-1515. IEEE, 2011.

[5] Rafael F. Rincon, T. Fatoyinbo, K. J. Ranson, G. Sun, M. Deshpande, M. Perrine, C. Du Toit et al. "ECOSAR'S PERFORMANCE ASSESSMENT AND FIRST FLIGHT CAMPAIGN RESULTS". In *Geoscience and Remote Sensing Symposium (IGARSS), 2014 IEEE International*. IEEE, 2014.

[6] J. Capon, "High-resolution frequency-wavenumber spectrum analysis," Proc. IEEE, vol. 57, pp.1408-1418 Aug. 1997

[7] R. o. Schmidt, "Multiple Emitter Location and Signal Parameter - Estimation," IEEE Trans. Antennas Propagat, vol. AP-34, pp. 276-280, Mar. 1986

[8] Godara, L. C., Smart Antennas, CRC Press, 2004.

[9] F. J. Meyer, J. B. Nicoll, and A. P. Doulgeris. "Correction and characterization of radio frequency interference signatures in L-band synthetic aperture radar data." *Geoscience and Remote Sensing, IEEE Transactions on* 51, no. 10 (2013): 4961-4972.

[10] G. A. Fabrizio, A. B. Gershman, and M. D. Turley. "Robust adaptive beamforming for HF surface wave over-the-horizon radar." *Aerospace and Electronic Systems, IEEE Transactions on* 40, no. 2 (2004): 510-525.

[11] L. Rosenberg, and D. Gray. "Anti-jamming techniques for multichannel SAR imaging." *IEE Proceedings-Radar, Sonar and Navigation* 153, no. 3 (2006): 234-242.